

# Observation of modulation-induced Feshbach resonance

Tongkang Wang,<sup>1,2</sup> Yuqi Liu,<sup>2</sup> Jundong Wang,<sup>2</sup> Youjia Huang,<sup>2</sup>  
Wenlan Chen,<sup>2,3,\*</sup> Zhendong Zhang,<sup>4,†</sup> and Jiazhong Hu<sup>1,‡</sup>

<sup>1</sup>*Beijing Academy of Quantum Information Sciences, Beijing 100193, China*

<sup>2</sup>*Department of Physics and State Key Laboratory of Low Dimensional  
Quantum Physics, Tsinghua University, Beijing, 100084, China*

<sup>3</sup>*Frontier Science Center for Quantum Information and Collaborative  
Innovation Center of Quantum Matter, Beijing, 100084, China*

<sup>4</sup>*Department of Physics and Hong Kong Institute of Quantum Science and Technology,  
The University of Hong Kong, Hong Kong, China*

In this work, we observe a novel resonant mechanism, namely the modulation-induced Feshbach resonance. By applying a far-detuned laser to the cesium  $D_2$  transition with intensity modulation, we periodically shake the energy levels of atomic collisional states. This periodic shaking connects the free-scattering states to shallow molecular states. At specific frequencies, we observe significant atom loss, which corresponds to the resonant coupling between these two types of states. This precisely corresponds to a form of Feshbach resonance, yet in the frequency domain rather than the magnetic-field domain. Using this method, we can directly scan the energy spectrum of molecular bound states without synthesizing any molecules. In addition to these bound states, we can also probe the molecular states embedded in the continuum, which are typically very difficult to detect by the conventional methods based on molecular synthesis. Moreover, by using a far-detuned laser instead of a magnetic field coil, it enables spatially dependent control over atomic interactions, coupling multiple levels simultaneously, and inducing new Feshbach resonances for those atoms that do not have conventional magnetic resonances. Therefore, we believe that this new resonant mechanism offers new opportunities for controlling atomic and molecular interactions in quantum simulations.

The Feshbach resonance [1] is a powerful tool in quantum many-body physics. By tuning the magnetic field, two energy levels of atomic or molecular collisional states can cross and couple with each other, leading to the divergence of scattering lengths. This resonant divergence provides a method to adjust the scattering length of ultracold atoms or molecules. Moreover, numerous new quantum phenomena have emerged through the utilization of quantum control techniques based on the Feshbach resonance [2, 3]. Following this logic, the quantum control community always demands a more versatile tool for adjusting collisional properties, as it may enable the creation of more novel quantum matters [4–27]. The conventional Feshbach resonance [1] is based on the adjustment of the magnetic field. However, it is sometimes challenging to locally address the field or rapidly switch the field direction or magnitude. This is because the magnetic field is created by current coils, which are on a centimeter- or millimeter-scale and have a large inductance that blocks AC oscillations [12–14]. Beyond the conventional method, several tools have been developed to control the Feshbach resonance, such as the optical Feshbach resonance [22–24], electric-field-linked resonance [25–27], and so on. Each method has unique advantages in controlling atomic and molecular interactions and creating numerous new matters. Recently, a new type of Feshbach resonance induced by magnetic modulation [28, 29] has been proposed.

Following this novel concept, we first theoretically extend this idea to a more generalized scenario. Sub-

sequently, we demonstrate this new phenomenon, the modulation-induced Feshbach resonance, by employing a far-detuned laser instead of a magnetic field coil. In previous studies [28, 29], this new resonance was based on the modulation of the scattering length. According to the Floquet theory, an AC-oscillating scattering length can enhance the DC interaction strength. By tuning the modulation frequency, it is anticipated that the effective scattering length will also diverge with respect to the frequency, which is highly similar to the conventional Feshbach resonance. A prerequisite for this modulated scattering length is the same as that of the conventional resonance: two energy levels must cross at a particular magnetic field [2, 28, 29], and any change around this specific resonant field will lead to a change in the scattering length. However, we have discovered that the pre-existence of a two-level crossing or a Feshbach resonance is not a mandatory requirement. The two energy levels of the collisional states do not need to cross with each other. All we need to do is applying a small periodic shaking to one of the energy levels, such that its energy oscillates slightly around its original value. Then, the Floquet theory can induce a new resonance between these two levels, which will directly result in the same behavior as the conventional Feshbach resonance. This provides a new way to tune the scattering length of atoms that do not have Feshbach resonances in the applicable magnetic fields.

In addition to the theoretical expansions, we conduct experimental demonstrations of this phenomenon using cesium atoms. Here, the energy level shaking is induced

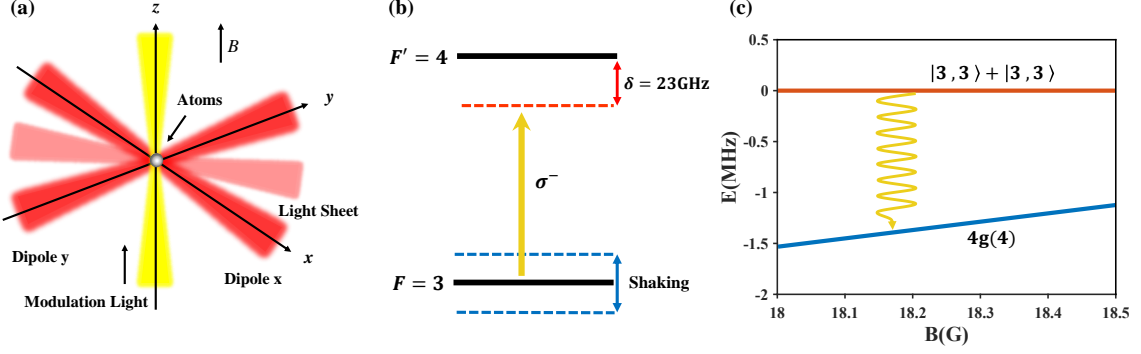


FIG. 1. (a) Experimental setup. We prepare a Bose-Einstein condensate with approximately  $10^5$  cesium atoms in the hyperfine state of  $|F = 3, m_F = 3\rangle$ . The condensate is trapped by a light sheet plus a cross-dipole trap in the  $x$ - $y$  plane, and the magnetic field is applied along the  $z$  axis. A 23-GHz-detuned light is sent along the  $z$  axis with a left-hand circular polarization as depicted in panel (b). This light has an intensity modulation with a modulation frequency  $\omega$ , which oscillates the differential energy shift between atomic collisional states and couples the free-scattering states to the molecular states such as  $4g(4)$  in panel (c).

by the intensity modulation of a far-detuned laser, which oscillates the energy difference between atomic collisional states. Specifically, we illustrate that the free-scattering states of two atoms in the  $|F = 3, m_F = 3\rangle$  state can exhibit frequency-based resonances with the molecular states  $4g(4)$ ,  $4d$  and  $6s$  and a near-frequency-independent resonance with  $6g(6)$ . These molecular states are characterized by the quantum numbers  $fl(m_f)$  [30], where  $f$  denotes the resultant of the total atomic angular momentum of the individual atoms,  $l$  is the orbital angular momentum of the relative motion, and  $m_f$  represents the projection of  $f$  along the quantization axis. For states with  $m_f = f$ , we omit  $(m_f)$  for brevity. This discovery leads to two novel advantages. First, we can directly scan out most of the shallow molecular states of cesium atoms, a result that will be presented in the subsequent sections of this manuscript, including those states in the continuum. Second, in principle, we can simultaneously apply multiple frequencies to modulate the laser intensity, enabling us to bring together many energy levels (more than two) to induce this resonance. Although this might seem conceptually straightforward, it is comparable to the scenarios of two-level and three-level systems in quantum optics. A three-level system is far more complex than a two-level one, as electromagnetic-induced transparency can only occur in a three-level (or multi-level) system. Moreover, numerous quantum applications [31–37] are based on this three-level structure. Therefore, the same reasoning applies to the Feshbach resonance. A recent observation of electromagnetic-induced loss suppression [31] under the Feshbach resonance and associated atomic collisions serves as supporting evidence, suggesting the potential for tunable interactions involving more levels.

Now we demonstrate how we extend the idea of the modulated magnetic Feshbach resonance using a two-

level model. This approach retains the essential physics while neglecting microscopic details of the scattering interactions. Assume we have two states,  $|\alpha\rangle$  and  $|\beta\rangle$ , with corresponding uncoupled energies  $\hbar\omega_\alpha$  and  $\hbar\omega_\beta$ , where  $\hbar$  is the reduced Planck constant, and define  $\omega_b = \omega_\alpha - \omega_\beta$  to denote the energy difference. There exists a non-zero off-diagonal coupling term  $\hbar\Omega/2$  between these two states due to non-zero wave function overlap. Without loss of generality, we consider that the energy of  $|\beta\rangle$  is periodically shaken in the form of  $\hbar\omega_\beta + \hbar A \cos(\omega t)$ , where  $A$  is the shaking amplitude and  $\omega$  is the shaking frequency. This shaking term  $\hbar A \cos(\omega t)$  can stem from the differential light shift between these two states caused by an intensity-modulated light. We can write the Hamiltonian  $H_0(t)$  in matrix form as:

$$H_0(t) = \hbar \begin{pmatrix} \omega_\alpha & \Omega/2 \\ \Omega/2 & \omega_\beta + A \cos(\omega t) \end{pmatrix}. \quad (1)$$

To transform this original Hamiltonian into a rotating frame, we apply a unitary transformation  $U(t)$ . The new Hamiltonian under transformation is  $H_1(t) = U(t)H_0(t)U^\dagger(t) - i\hbar U(t)\partial U^\dagger(t)/\partial t$ . When choose  $U(t)$  in the diagonal form  $U(t) = \text{Diag}\{1, e^{i[m\omega t + \frac{A}{\omega} \sin(\omega t)]}\}$ , where  $m$  is an integer,  $H_1(t)$  becomes:

$$H_1(t) = \hbar \begin{pmatrix} \omega_\alpha & \frac{\Omega}{2} e^{-i[m\omega t + \frac{A}{\omega} \sin(\omega t)]} \\ \frac{\Omega}{2} e^{i[m\omega t + \frac{A}{\omega} \sin(\omega t)]} & \omega_\alpha - \omega_b - m\omega \end{pmatrix}. \quad (2)$$

By using the expansion  $e^{i\frac{A}{\omega} \sin(\omega t)} = \sum_n J_n(A/\omega) e^{in\omega t}$ , where  $J_n(x)$  is the  $n$ -th order Bessel function of the first

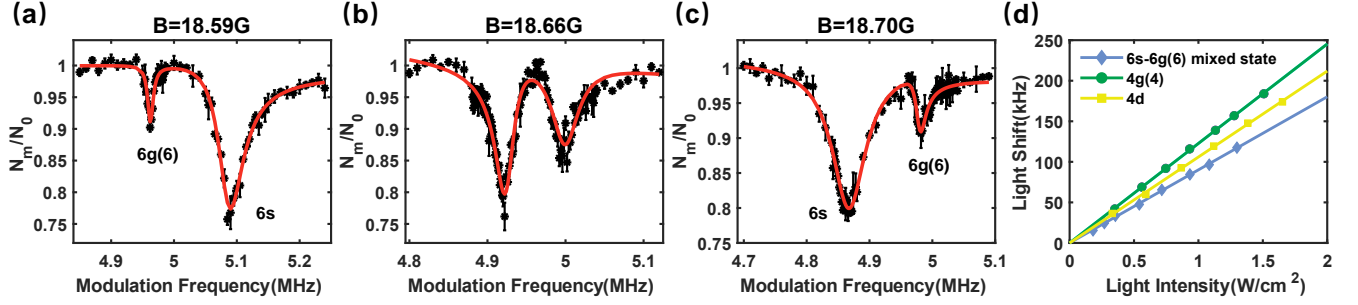


FIG. 2. Typical atom loss signals in the frequency domain and dependence of the resonance position shift on the average peak intensity. In (a)-(c), we show the relative atom number  $N_m/N_0$  versus the modulation frequency  $\omega$  after 5 ms exposure to  $0.86 \text{ W/cm}^2$  (average peak intensity) modulation light at 18.59 G, 18.66 G and 18.70 G, respectively. We also label about the resonant peaks with corresponding molecular states  $6g(6)$  and  $6s$  in panels (a) and (c), while these two molecular states are strongly mixed in panel (b). The experimental atom loss signal (dark solid circle) in each panel is fitted with a Fano profile (red solid lines), and all error bars represents one standard deviation of measurements. In panel (d), we present a linear fitting example of the resonance position shift caused by the DC component of the light intensity for  $4g(4)$ ,  $4d$  molecular states and one of the  $6s$ - $6g(6)$  mixed molecular states at respective magnetic field of 17.27 G, 47.36 G and 18.66 G, which offers a route to compensate the resonance frequency shift.

kind, we rewrite  $H_1$  as:

$$\frac{H_1(t)}{\hbar} = \omega_\alpha + \left( \begin{array}{cc} 0 & \sum_n \frac{\Omega}{2} J_n\left(\frac{A}{\omega}\right) e^{-i(m+n)\omega t} \\ \sum_n \frac{\Omega}{2} J_n\left(\frac{A}{\omega}\right) e^{i(m+n)\omega t} & -\omega_b - m\omega \end{array} \right) \quad (3)$$

The first term  $\omega_\alpha$  is a constant and can be ignored. The second term describes the interaction between the two states. By retaining the resonant term under the condition  $n = -m$ , we can simplify the interaction Hamiltonian to:

$$\frac{H_1(t)}{\hbar} - \omega_\alpha = \left( \begin{array}{cc} 0 & \frac{\Omega}{2} (-1)^m J_m\left(\frac{A}{\omega}\right) \\ \frac{\Omega}{2} (-1)^m J_m\left(\frac{A}{\omega}\right) & -\omega_b - m\omega \end{array} \right). \quad (4)$$

Therefore, when  $m\omega$  approaches  $-\omega_b = \omega_\beta - \omega_\alpha$ , the system becomes a resonant-coupled two-level system. Detailed derivations of its effects on scattering properties and scattering lengths are provided in the Supplementary Materials [38]. Here, we present the conclusion that due to the resonant coupling from  $|\alpha\rangle$  to  $|\beta\rangle$ , the effective scattering length  $a_s$  of the incoming state  $|\alpha\rangle$  has the form:

$$a_s = a_{\text{BK}} \left( 1 - \frac{\Delta_m}{-m\omega - \omega_0} \right). \quad (5)$$

Here  $a_{\text{BK}}$  is the background scattering length,  $\Delta_m$  is the width of the resonance and  $\omega_0$  is close to  $\omega_b$ . It exactly corresponds to the form of Feshbach resonance, but with the magnetic field replaced by an integer multiple of the modulation frequency  $\omega$ , which we use the term, modulation-induced Feshbach resonance, to describe it. Comparing to the previous study by modulating the scattering length, here the two energy levels  $|\alpha\rangle$  and  $|\beta\rangle$  do

not need any crossing or preexisted Feshbach resonance, as it only need tiny level shaking.

We now turn to the experimental implementation. We prepare a Bose-Einstein condensate consisting of approximately  $10^5$  cesium atoms, with all atoms initialized in the  $6S$  hyperfine ground state  $|F = 3, m_F = 3\rangle$  [38]. A magnetic field  $B$  is applied along the  $z$ -axis (as depicted in Fig. 1a) and serves as the quantization axis. Subsequently, an intensity-modulated light with a left-hand circularly polarization and a 23 GHz red-detuning relative to the cesium  $D_2$  transition of  $F = 3 \rightarrow F' = 4$  (Fig. 1b), is directed along the  $z$ -axis towards the atoms, inducing the light shift on the free-scattering states and

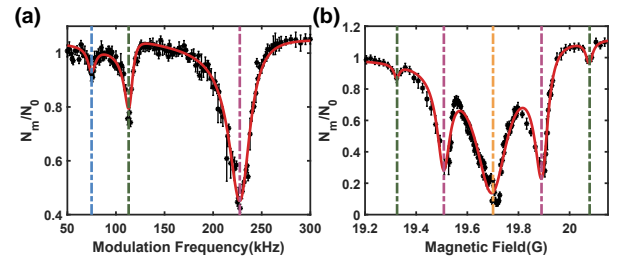


FIG. 3. Multiple resonances of the  $4g(4)$  molecular state. (a) Sweeping the modulation frequency at 19.41 G, we observe three distinct atom loss peaks, located at 228.7 kHz, 114.3 kHz, and 75.0 kHz, corresponding to the first-, second-, and third-order resonance frequencies of the  $4g(4)$  state, respectively. (b) Magnetic field scan under a fixed modulation frequency of 150 kHz, reveals an optically shifted Feshbach resonance at 19.70 G, along with the first- and second-order modulation resonances located at 19.51 G, 19.32 G (left side), 19.90 G and 20.08 G (right side), respectively. The average peak intensity of used modulation light in both two panels is  $0.87 \text{ W/cm}^2$ .

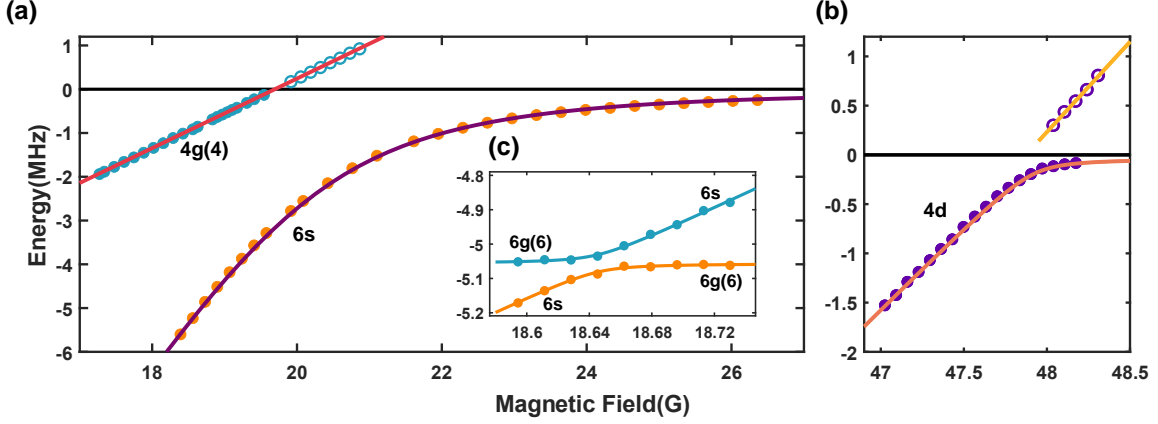


FIG. 4. The energy spectrum of cesium molecular states. We plot the modulation frequencies  $\omega$  (or energies) versus the magnetic fields  $B$ . The vertical axis is plotted upside down in order to provide the same illustration of the bound state plot. Here, we use filled symbols to plot data corresponding to molecular bound states whose energy is lower than 0, and we use unfilled symbols to plot data corresponding to molecular states in the continuum whose energy is higher than 0. The black solid line along  $\omega = 0$  corresponds to the free-scattering states. The other solid lines are the theoretical models calculated for molecular states  $6g(6)$ ,  $6s$ ,  $4g(4)$  and  $4d$ . The  $4g(4)$  and  $4d$  data are obtained at a average peak intensity  $0.86 \text{ W/cm}^2$  with corresponding theoretical lines shifted from their original Feshbach resonance points to the optically shifted ones measured in experiments, while the  $6s$  and  $6g(6)$  data are obtained by varying the average peak intensity and compensating the DC component of the light shift by linear fitting.

molecular states [38]. The average peak intensity is varied from  $0.2 \text{ W/cm}^2$  to  $1.7 \text{ W/cm}^2$  in our experiments, while the modulation depth is fixed to be 86%. Then we vary the modulation frequencies  $\omega$  with the aim of coupling the molecular states (Fig. 1c). After irradiating the atoms with the light for 1-20 ms, we switch off the light and measure the remaining atom number [15].

In Fig. 2a-c, we present data obtained at different magnetic fields (18.59, 18.66, and 18.70 G). Here the modulation-induced resonances are exhibited by the significant atom loss signals of the relative atom number  $N_m/N_0$ , where  $N_m$  is the remaining atom number after modulation, and  $N_0$  is the atom number far away from resonance positions. These loss signals correspond to the molecular state  $6s$  and  $6g(6)$ . Especially, the energy level of  $6g(6)$  is nearly parallel to the incoming scattering state (both atoms in  $|F = 3, m_F = 3\rangle$ ) as a function of the magnetic field, and this state does not have a direct energy crossing with the scattering state at low magnetic field regime [39]. These experimental results confirm our hypothesis that modulation can induce a resonance between two states without the pre-existence of a conventional Feshbach resonance. Furthermore, we also observe other atom loss features correspond to the molecular states  $4g(4)$  and  $4d$ , and their resonant frequencies exhibit obvious dependence on the magnetic field like the molecular state  $6s$ . Notably, the measured atom loss peaks are all red-shifted due to the unequal DC component of the light shift between the free-scattering states and the molecular states. This shift can be determined and compensated by way of linearly fitting between the

atom loss peak position and the average peak intensity, as shown in Fig. 2d. The atom-loss characteristics as a function of frequency precisely mirror the form of the conventional Feshbach resonance, where atom-loss features are measured as a function of the magnetic field. This type of resonance in the frequency domain is what we term the modulation-induced Feshbach resonance.

In most cases, there is only one resonance peak for each molecular state, which corresponds to the first-order modulation resonance for  $|m| = 1$  in Eq. (5) ( $m = -1$  for molecular states below the atomic scattering threshold,  $m = 1$  for molecular states above the atomic scattering threshold). However, when the shaking amplitude  $A$  is comparable to the  $|m| > 1$  multiple of the energy difference  $\omega_b$  between the free-scattering state and the molecular state, the higher-order modulation resonances emerge. For the  $4g(4)$  molecular state at magnetic fields where the binding energy is relatively small, we clearly observe these higher-order resonances. As exhibited in Fig. 3a, the dominant loss peak at  $f_1 = 228.7 \text{ kHz}$  (purple dash-dotted line) corresponds to the first-order modulation resonance at 19.41 G. The peaks at frequencies  $f_2 = 114.3 \text{ kHz} \approx f_1/2$  and  $f_3 = 75.0 \text{ kHz} \approx f_1/3$  indicate the higher-order modulation resonances (green and blue dash-dotted lines). Moreover, these modulation effects actually also modified the atom-loss feature as a function of the magnetic field, which can be understood by fixing the modulation frequency  $\omega$  and varying the  $\omega_0$  with the magnetic field in Eq. (5). We show these effects in Fig. 3b by sweeping the magnetic field and measuring the relative atom number  $N_m/N_0$  at a fixed modulation

frequency of 150 kHz. Surprisingly, the Feshbach resonance is significantly shifted from 19.84 G to 19.70 G (orange dash-dotted line) due to the light shift [38]. The peaks at 19.51 G and 19.90 G (purple dash-dotted line) are attributed to the first-order modulation resonances, while those at 19.32 G and 20.08 G (green dash-dotted line) arise from the second-order modulation resonances. The resonance features appearing at the left side of the shifted Feshbach resonance arise from coupling between free-scattering states and bound molecular states, while those at the right side result from coupling between free-scattering states and the molecular states embedded in the continuum.

In Fig. 4, we plot the measured resonant frequencies as a function of the magnetic field. Simultaneously, we plot the theoretical values [30, 39, 40] of these molecular states for comparison (solid lines). The vertical axis of the modulation frequency  $\omega$  is inverted for the bound states whose energies are below those of the free-scattering states. In addition to the bound states, we also identify the molecular states embedded in the continuum. The unfilled symbols in the plot represent our measurement results for these states in the continuum. Our experimental data (mainly shifted by the DC component of the light intensity) reveal the  $6g(6)$ ,  $6s$ ,  $4d$ , and  $4g(4)$  molecular states. By comparing experimental data with theoretical calculations, we observe excellent agreement between them, demonstrating the effectiveness of our method for probing these molecular states.

Beyond the overall view of the energy spectrum, there are also intriguing detailed features observable in this plot. In Fig. 4c, we zoom in on the crossing region of the  $6g(6)$  and  $6s$  states, where the states are obtained by eliminating the light shift. This region exhibits the characteristic features of a Landau-Zener crossing, where two energy levels intersect and a coupling term between them creates an energy gap. By fitting the data to the Landau-Zener model where the energies are decided by  $E_{\pm} = [E_i + E_j \pm \sqrt{(E_i - E_j)^2 + V_{ij}^2}] / 2$ , we determine that the Rabi frequency  $V_{ij}/\hbar$  of this coupling between these two states is 25 kHz.

In conclusion, we have experimentally observed a novel resonant mechanism, the modulation-induced Feshbach resonance, through the utilization of an intensity-modulated light. This new resonance shares a similar form with the conventional Feshbach resonance, yet it occurs in the frequency domain rather than relying on a tunable magnetic field. It enables us to directly map out the energy spectrum of shallow molecular states, including those embedded in the continuum. Given the highly versatile tunability of lasers, in principle, we can bring together more than two energy levels to induce the resonance, which we anticipate will surpass the capabilities of the conventional Feshbach resonance. We look forward to the further development of future experimen-

tal investigations and associated applications based on a three-level resonance.

This work is supported by the National Natural Science Foundation of China and the National Key Research and Development Program of China.

---

\* cwllaser@ultracold.cn

† zhendongzhang19950715@gmail.com

‡ hujiazhong01@ultracold.cn

- [1] S. Inouye, M. R. Andrews, J. Stenger, H. J. Miesner, D. M. Stamper-Kurn, and W. Ketterle, Observation of Feshbach resonances in a Bose-Einstein condensate, *Nature* **392**, 151 (1998).
- [2] C. Chin, R. Grimm, P. Julienne, and E. Tiesinga, Feshbach resonances in ultracold gases, *Rev. Mod. Phys.* **82**, 1225 (2010).
- [3] I. Bloch, J. Dalibard, and W. Zwerger, Many-body physics with ultracold gases, *Rev. Mod. Phys.* **80**, 885 (2008).
- [4] T. Kraemer, M. Mark, P. Waldburger, J. G. Danzl, C. Chin, B. Engeser, A. D. Lange, K. Pilch, A. Jaakkola, H. C. Nägerl, and R. Grimm, Evidence for Efimov quantum states in an ultracold gas of caesium atoms, *Nature* **440**, 315 (2006).
- [5] E. Haller, M. Gustavsson, M. J. Mark, J. G. Danzl, R. Hart, G. Pupillo, and H.-C. Nägerl, Realization of an excited, strongly correlated quantum gas phase, *Science* **325**, 1224 (2009).
- [6] K.-K. Ni, S. Ospelkaus, M. H. G. de Miranda, A. Pe'er, B. Neyenhuis, J. J. Zirbel, S. Kotochigova, P. S. Julienne, D. S. Jin, and J. Ye, A high phase-space-density gas of polar molecules, *Science* **322**, 231 (2008).
- [7] L. Liang, W. Zheng, R. Yao, Q. Zheng, Z. Yao, T.-G. Zhou, Q. Huang, Z. Zhang, J. Ye, X. Zhou, X. Chen, W. Chen, H. Zhai, and J. Hu, Probing quantum many-body correlations by universal ramping dynamics, *Science Bulletin* **67**, 2550 (2022).
- [8] L. R. Liu, J. D. Hood, Y. Yu, J. T. Zhang, N. R. Hutzler, T. Rosenband, and K.-K. Ni, Building one molecule from a reservoir of two atoms, *Science* **360**, 900 (2018).
- [9] H. Yang, X.-Y. Wang, Z. Su, J. Cao, D.-C. Zhang, J. Rui, B. Zhao, C.-L. Bai, and J.-W. Pan, Evidence for the association of triatomic molecules in ultracold  $^{23}\text{Na}^{40}\text{K} + ^{40}\text{K}$  mixtures, *Nature* **602**, 229 (2022).
- [10] S. Miao, Z. Zhang, Y. Zhao, Z. Zhao, H. Wang, and J. Hu, Bosonic fractional quantum Hall conductance in shaken honeycomb optical lattices without flat bands, *Phys. Rev. B* **106**, 054310 (2022).
- [11] J. J. Park, Y.-K. Lu, A. O. Jamison, T. V. Tscherbul, and W. Ketterle, A Feshbach resonance in collisions between triplet ground-state molecules, *Nature* **614**, 54 (2023).
- [12] J. Hu, L. Feng, Z. Zhang, and C. Chin, Quantum simulation of Unruh radiation, *Nature Physics* **15**, 785 (2019).
- [13] L. Feng, J. Hu, L. W. Clark, and C. Chin, Correlations in high harmonic generation of matter-wave jets revealed by pattern recognition, *Science* **524**, 521 (2019).
- [14] Z. Zhang, K.-X. Yao, L. Feng, J. Hu, and C. Chin, Pattern formation in a driven Bose-Einstein condensate, *Nature Physics* **16**, 652 (2020).
- [15] Y. Liu, Z. Zhang, S. Miao, Z. Zhao, H. Wang, W. Chen,



- and J. Hu, Calibrating the absorption imaging of cold atoms under high magnetic fields, *Phys. Rev. Appl.* **20**, 014037 (2023).
- [16] T. M. Hanna, T. Köhler, and K. Burnett, Association of molecules using a resonantly modulated magnetic field, *Phys. Rev. A* **75**, 013606 (2007).
- [17] Y. Zhao, R. Zhang, W. Chen, X.-B. Wang, and J. Hu, Creation of Greenberger-Horne-Zeilinger states with thousands of atoms by entanglement amplification, *npj Quantum Information* **7**, 24 (2021).
- [18] V. Venu, P. Xu, M. Mamaev, F. Corapi, T. Bilitewski, J. P. D’Incao, C. J. Fujiwara, A. M. Rey, and J. H. Thywissen, Unitary p-wave interactions between fermions in an optical lattice, *Nature* **613**, 262 (2023).
- [19] Q. Huang, R. Yao, L. Liang, S. Wang, Q. Zheng, D. Li, W. Xiong, X. Zhou, W. Chen, X. Chen, and J. Hu, Observation of many-body quantum phase transitions beyond the kibble-zurek mechanism, *Phys. Rev. Lett.* **127**, 200601 (2021).
- [20] H. Yang, J. Cao, Z. Su, J. Rui, B. Zhao, and J.-W. Pan, Creation of an ultracold gas of triatomic molecules from an atom-diatom molecule mixture, *Science* **378**, 1009 (2022).
- [21] T. Zhang, Z. Chi, and J. Hu, Entanglement generation via single-qubit rotations in a torn hilbert space, *PRX Quantum* **5**, 030345 (2024).
- [22] M. Theis, G. Thalhammer, K. Winkler, M. Hellwig, G. Ruff, R. Grimm, and J. H. Denschlag, Tuning the scattering length with an optically induced Feshbach resonance, *Phys. Rev. Lett.* **93**, 123001 (2004).
- [23] D. M. Bauer, M. Lettner, C. Vo, G. Rempe, and S. Dürr, Control of a magnetic Feshbach resonance with laser light, *Nature Physics* **5**, 339 (2009).
- [24] L. W. Clark, L.-C. Ha, C.-Y. Xu, and C. Chin, Quantum dynamics with spatiotemporal control of interactions in a stable Bose-Einstein condensate, *Phys. Rev. Lett.* **115**, 155301 (2015).
- [25] X.-Y. Chen, A. Schindewolf, S. Eppelt, R. Bause, M. Duda, S. Biswas, T. Karman, T. Hilker, I. Bloch, and X.-Y. Luo, Field-linked resonances of polar molecules, *Nature* **614**, 59 (2023).
- [26] L. Lassablière and G. Quémener, Controlling the scattering length of ultracold dipolar molecules, *Phys. Rev. Lett.* **121**, 163402 (2018).
- [27] X.-Y. Chen, S. Biswas, S. Eppelt, A. Schindewolf, F. Deng, T. Shi, S. Yi, T. A. Hilker, I. Bloch, and X.-Y. Luo, Ultracold field-linked tetratomic molecules, *Nature* **626**, 283 (2024).
- [28] C. Langmack, D. H. Smith, and E. Braaten, Association of atoms into universal dimers using an oscillating magnetic field, *Phys. Rev. Lett.* **114**, 103002 (2015).
- [29] D. H. Smith, Inducing resonant interactions in ultracold atoms with a modulated magnetic field, *Phys. Rev. Lett.* **115**, 193002 (2015).
- [30] M. Mark, F. Ferlaino, S. Knoop, J. G. Danzl, T. Kraemer, C. Chin, H.-C. Nägerl, and R. Grimm, Spectroscopy of ultracold trapped cesium Feshbach molecules, *Phys. Rev. A* **76**, 042514 (2007).
- [31] A. Jagannathan, N. Arunkumar, J. A. Joseph, and J. E. Thomas, Optical control of magnetic Feshbach resonances by closed-channel electromagnetically induced transparency, *Phys. Rev. Lett.* **116**, 075301 (2016).
- [32] H. Tanji-Suzuki, W. Chen, R. Landig, J. Simon, and V. Vuletić, Vacuum-induced transparency, *Science* **333**, 1266 (2011).
- [33] W. Chen, K. M. Beck, R. Bücke, M. Gullans, M. D. Lukin, H. Tanji-Suzuki, and V. Vuletić, All-optical switch and transistor gated by one stored photon, *Science* **341**, 768 (2013).
- [34] S. Sun, H. Kim, Z. Luo, G. S. Solomon, and E. Waks, A single-photon switch and transistor enabled by a solid-state quantum memory, *Science* **361**, 57 (2018).
- [35] D. Niemietz, P. Farrera, S. Langenfeld, and G. Rempe, Nondestructive detection of photonic qubits, *Nature* **591**, 570 (2021).
- [36] A. Kuhn, M. Hennrich, and G. Rempe, Deterministic single-photon source for distributed quantum networking, *Phys. Rev. Lett.* **89**, 067901 (2002).
- [37] Y. Wang, J. Li, S. Zhang, K. Su, Y. Zhou, K. Liao, S. Du, H. Yan, and S.-L. Zhu, Efficient quantum memory for single-photon polarization qubits, *Nature Photonics* **13**, 346 (2019).
- [38] Supplementary material, (2025).
- [39] M. Berninger, A. Zenesini, B. Huang, W. Harm, H.-C. Nägerl, F. Ferlaino, R. Grimm, P. S. Julienne, and J. M. Hutson, Feshbach resonances, weakly bound molecular states, and coupled-channel potentials for cesium at high magnetic fields, *Phys. Rev. A* **87**, 032517 (2013).
- [40] A. D. Lange, K. Pilch, A. Prantner, F. Ferlaino, B. Engeser, H.-C. Nägerl, R. Grimm, and C. Chin, Determination of atomic scattering lengths from measurements of molecular binding energies near feshbach resonances, *Phys. Rev. A* **79**, 013622 (2009).

# Supplementary Material for: Observation of modulation-induced Feshbach resonance

Tongkang Wang,<sup>1,2</sup> Yuqi Liu,<sup>2</sup> Jundong Wang,<sup>2</sup> Youjia Huang,<sup>2</sup>  
Wenlan Chen,<sup>2,3,\*</sup> Zhendong Zhang,<sup>4,†</sup> and Jiazhong Hu<sup>1,‡</sup>

<sup>1</sup>*Beijing Academy of Quantum Information Sciences, Beijing 100193, China*

<sup>2</sup>*Department of Physics and State Key Laboratory of Low Dimensional  
Quantum Physics, Tsinghua University, Beijing, 100084, China*

<sup>3</sup>*Frontier Science Center for Quantum Information and Collaborative  
Innovation Center of Quantum Matter, Beijing, 100084, China*

<sup>4</sup>*Department of Physics and Hong Kong Institute of Quantum Science and Technology,  
The University of Hong Kong, Hong Kong, China*

## EXPERIMENTAL SETUP

Most of our experiments begin by preparing an almost pure Bose-Einstein condensate (BEC) of approximately  $10^5$  cesium atoms in the hyperfine state  $|3, 3\rangle$ . These atoms are confined in an optical trap consisting of a light sheet and a cross-dipole trap formed by a 1064-nm laser in the  $x$ - $y$  plane. Under a uniform magnetic field, the typical trap frequencies are  $\omega_z = 2\pi \times 65$  Hz (vertical) and  $\omega_r = 2\pi \times 28$  Hz (horizontal). The final evaporation field is set to 20.8 G, where the scattering length is small and positive ( $a = 200 a_0$ ). We then ramp the magnetic field to a target value (stable to within 4 mG, calibrated via microwave) and switch on the modulation light. After an optimized hold time (1–20 ms), we simultaneously extinguish the light and ramp the field back to 20.8 G for expansion and imaging. Finally, absorption imaging measures the remaining atom number after 18 ms of time-of-flight.

Light intensity modulation is achieved through the interference of two laser beams, each passing through a separate acousto-optic modulator (AOM) operating at different frequencies, combined by a beam splitter. The variation of light intensity over time is measured by a biased Silicon detector with the band width about 80 MHz, which shows that the modulation depth is about 86%, while the half-width of modulation frequency is lower than 1 Hz. The beam waist of modulation light is chosen to be  $844 \mu\text{m}$ , which is much larger than the typical Bose-Einstein condensate size, and the average peak intensity is ranged from  $0.2 \text{ W/cm}^2$  to  $1.7 \text{ W/cm}^2$  according to experimental requirements.

When scanning the energy spectrum in the main text, the binding energy detection for the  $4g4$ ,  $6s$ , and  $6g(6)$  states starts from an almost pure Bose-Einstein condensate as described above. However, since the scattering length is  $\sim 900 a_0$  in the region of 47–48.5 G, the  $4d$  data are measured by initializing a mixture of Bose-Einstein condensate and thermal atoms to reduce three-body recombination losses, which improves the signal-to-noise ratio of atom loss peaks.

## LIGHT SHIFT OF FREE-SCATTERING STATES AND MOLECULAR STATES

In our experiments, the 23 GHz red-detuned,  $\sigma^-$ -polarized light generates different light shifts on the free scattering state of two atoms in the  $|F = 3, m_F = 3\rangle$  state and the molecular states, as described in the main text. Especially, the Feshbach resonance at 19.84 G is shifted to 19.70 G under a  $0.87 \text{ W/cm}^2$  peak intensity light (the shift is same for the light without modulation). The observed 140 mG shift is beyond the region where the shift is mainly attributed to the fictitious magnetic field as reported in [1] with a much larger detuning light.

To make a comparison, we calculate the fictitious magnetic field [2, 3] :

$$\mathbf{B}_z^f = -\frac{I\mu_0 c}{2\mu_B g_F F} (|\mathbf{u}_{-1}|^2 - |\mathbf{u}_{+1}|^2) \alpha_v, \quad (1)$$

where  $I$  is the intensity of light,  $\mu_0$  is the vacuum permeability,  $c$  is the speed of light,  $\mu_B$  is the Bohr magneton,  $g_F$  is the hyperfine Landé g-factor,  $\mathbf{u} = \sum_{q=0,\pm 1} (-1)^q \mathbf{u}_q \hat{e}_{-q}$  is the complex unit vector,  $\hat{e}_{\pm 1} = \mp \frac{1}{\sqrt{2}} (\hat{e}_x \pm i\hat{e}_y)$ ,  $\hat{e}_0 = \hat{e}_z$  are the spherical basis vectors in terms of the Cartesian basis vectors  $\hat{e}_x$ ,  $\hat{e}_y$  and  $\hat{e}_z$ , and  $\mathbf{u}_{\pm 1} = \mp \frac{1}{\sqrt{2}} (\mathbf{u}_x \pm i\mathbf{u}_y)$ ,  $\mathbf{u}_0 = \mathbf{u}_z$  are the spherical components of  $\mathbf{u}$  in terms of the Cartesian components  $\mathbf{u}_x$ ,  $\mathbf{u}_y$  and  $\mathbf{u}_z$ ,  $\alpha_v$  is the vector polarizability such that

$$\alpha_v(F; \omega) = \sum_{F'} (-1)^{F+F'+1} \sqrt{\frac{6F(2F+1)}{F+1}} \begin{Bmatrix} 1 & 1 & 1 \\ F & F & F' \end{Bmatrix} \frac{\omega |\langle J || \mathbf{d} || J' \rangle|^2}{\hbar(\omega_{F',F}^2 - \omega^2)} (2F' + 1)(2J + 1) \begin{Bmatrix} J & J' & 1 \\ F' & F & I \end{Bmatrix}^2, \quad (2)$$

where  $\omega$  is the angular frequency of light,  $\omega_{F'F}$  is the resonance frequency from hyperfine level  $F$  to  $F'$ ,  $\left\{ \begin{smallmatrix} j_1 & j_2 & j_3 \\ j_4 & j_5 & j_6 \end{smallmatrix} \right\}$  is the Wigner 6-j symbol,  $\hbar$  is the reduced Planck's constant,  $\mathbf{d}$  is the dipole operator,  $\langle J || \mathbf{d} || J' \rangle$  is the reduced matrix element,  $J$  is the electron angular momentum, and  $I$  is the nuclear spin momentum.

Since the frequency of our intensity-modulated light is detuned tens of GHz from the cesium D2 transition  $|F = 3\rangle \rightarrow |F' = 4\rangle$ , we only include the D1 and D2 transitions in our calculation, with all the relevant calculation parameters listed in Table I. Therefore, the calculated fictitious magnetic field generated by a 23GHz red-detuned,  $\sigma^-$  polarized and 0.87 W/cm<sup>2</sup> light is 35.6 mG.

	Transition	$\omega_{F'F}/2\pi$ (THz)	$\langle J    \mathbf{d}    J' \rangle$ (C · m)
D1	$F = 3 \rightarrow F' = 3$	335.12056284	$2.6980 \times 10^{-29}$
	$F = 3 \rightarrow F' = 4$	335.12173052	
D2	$F = 3 \rightarrow F' = 2$	351.73054972	$3.7971 \times 10^{-29}$
	$F = 3 \rightarrow F' = 3$	351.73070092	
	$F = 3 \rightarrow F' = 4$	351.73090217	

TABLE I: The used parameters for the calculation of  $F = 3$  states' fictitious magnetic field.

Moreover, we vary the polarization as well as detuning from -200 GHz to 50GHz in experiments, observing two intriguing results. Firstly, the Feshbach resonance shift caused by linear polarized light is on the same order of magnitude as  $\sigma^-$  case, which indicates that the scalar shift difference between the free-scattering state and the molecular states could not be neglected. Secondly, the shifted value decreases monotonically with the increasing detuning in blue detuned case, while it can dramatically change its sign at some detuning points in red detuned case. This behaviour may be attributed to the bound-bound transitions between the ground molecular states and the excited molecular states [4, 5]. Despite its complex details, it's sufficient for us to know that the collisional states can be distinctly shifted, so that we can realize the modulation-induced resonance.

## THE SCATTERING PROPERTIES OF MODULATION-INDUCED FESHBACH RESONANCE

To study the scattering properties of modulation-induced Feshbach resonances, we employ a two-channel model to simplify the problem. The system can be described by the Hamiltonian  $H_0 = H_{op} |op\rangle \langle op| + W(r) |op\rangle \langle cl| + W(r) |cl\rangle \langle op| + (H_{cl} + \hbar A \cos \omega t) |cl\rangle \langle cl|$ , where  $H_{op}$  and  $H_{cl}$  denote Hamiltonian for the open channel and the closed channel, respectively,  $W(r)$  is the coupling between them and  $A$  is the shaking amplitude as mentioned in the main text.

Subsequently, We take an unitary transformation  $H_1(t) = U(t)H_0(t)U^\dagger(t) - i\hbar U(t)\partial U^\dagger(t)/\partial t$ , and choose  $U(t)$  in the diagonal form  $U(t) = 1 |op\rangle \langle op| + e^{i[m\omega t + \frac{A}{\omega} \sin(\omega t)]} |cl\rangle \langle cl|$ , where  $m$  is an integer. As a result,  $H_1(t)$  becomes  $H_{op} |op\rangle \langle op| + W(r)e^{-i[m\omega t + \frac{A}{\omega} \sin(\omega t)]} |op\rangle \langle cl| + W(r)e^{i[m\omega t + \frac{A}{\omega} \sin(\omega t)]} |cl\rangle \langle op| + (H_{cl} - m\hbar\omega) |cl\rangle \langle cl|$ .

By using the expansion  $e^{i\frac{A}{\omega} \sin(\omega t)} = \sum_n J_n(A/\omega) e^{in\omega t}$ , where  $J_n(x)$  is the  $n$ -th order Bessel function of the first kind, and neglecting the high-frequency terms when the incident energy  $E$  approaches the resonance energy  $E_{res} = \hbar\omega_{cl} - m\hbar\omega$ , where  $\hbar\omega_{cl}$  is the molecular state energy in the closed channel with respect to the free-scattering states, we can simplify the Hamiltonian to  $H_1(t) = H_{op} |op\rangle \langle op| + (-1)^m W(r) J_m(A/\omega) |op\rangle \langle cl| + (-1)^m W(r) J_m(A/\omega) |cl\rangle \langle op| + (H_{cl} - m\hbar\omega) |cl\rangle \langle cl|$ . Under this Hamiltonian, we can determine the scattering properties by solving the following set of coupled stationary Schrödinger equations with the state  $\varphi_{op}(r) |op\rangle + \varphi_{cl}(r) |cl\rangle$  [6]:

$$\begin{cases} H_{op}\varphi_{op}(r) + (-1)^m J_m(A/\omega) W(r) \varphi_{cl}(r) = E \varphi_{op}(r) \\ (-1)^m J_m(A/\omega) W(r) \varphi_{op}(r) + (H_{cl} - m\hbar\omega) \varphi_{cl}(r) = E \varphi_{cl}(r) \end{cases}, \quad (3)$$

where  $\varphi_{op}(r)$  and  $\varphi_{cl}(r)$  represent the corresponding wave function of the state of open channel and closed channel. Notably,  $\varphi_{op}(r)$  has the standard asymptotic solution as:

$$\varphi_{op}(r)|_{r \rightarrow \infty} \sim \frac{1}{(2\pi)^{\frac{3}{2}}} (e^{i\mathbf{k} \cdot \mathbf{r}} + f(\theta, k) \frac{e^{ikr}}{r}) \quad (4)$$



Here,  $f(\theta, k)$  denotes the scattering amplitude,  $k$  is the incident wave vector, and  $\theta$  is the incident angle between  $\mathbf{k}$  and  $\mathbf{r}$ . And the cross section of scattering between two channels is described by  $|f(\theta, k)|^2$ . From the coupled Schrödinger equations in Eq. 3, we derive the Lippmann-Schwinger equation as:

$$\begin{cases} |\varphi_{op}\rangle = |\varphi_{\mathbf{k}}^{(+)}\rangle + (-1)^m G_{op}(E + i\eta^{0+}) J_m(A/\omega) W |\varphi_{cl}\rangle \\ |\varphi_{cl}\rangle = (-1)^m G_{cl}(E) J_m(A/\omega) W |\varphi_{op}\rangle \end{cases} \quad (5)$$

Where  $|\varphi_{\mathbf{k}}^{(+)}\rangle$  is the background scattering state, which satisfies  $H_{op} |\varphi_{\mathbf{k}}^{(+)}\rangle = \frac{\hbar^2 k^2}{2\mu} |\varphi_{\mathbf{k}}^{(+)}\rangle$ , where  $\mu$  is the reduced mass. The operators  $G_{op}$  and  $G_{cl}$  represent the Green's functions of the open channel and the closed channel, respectively, and are given by:

$$\begin{cases} G_{op}(E + i\eta^{0+}) = (E + i\eta^{0+} - H_{op})^{-1} \\ G_{cl}(E) = (E - H_{cl} + m\hbar\omega)^{-1} \end{cases} \quad (6)$$

As shown in Eq. 6, the Green's function of the closed channel  $G_{cl}$  exhibits a singularity at the resonance energy  $E_{res}$ , corresponding to the modulated-induced resonance discussed in the main text. Here we construct the state of resonance  $|\varphi_{res}\rangle$ , which satisfies the following relationship as:

$$\langle \varphi_{res} | G_{cl}(E) | \varphi_{res} \rangle = (E - E_{res})^{-1} \quad (7)$$

Based on this relation, we can approximate the Green's function of closed channel as:

$$G_{cl}(E) \approx |\varphi_{res}\rangle (E - E_{res})^{-1} \langle \varphi_{res} | \quad (8)$$

Therefore, by eliminating  $G_{cl}$ , we can reformulate the coupled Schrödinger equations using the factor  $D = \langle \varphi_{res} | (-1)^m J_m(A/\omega) W | \varphi_{cl} \rangle / (E - E_{res})$  as follow:

$$\begin{cases} |\varphi_{op}\rangle = |\varphi_{\mathbf{k}}^{(+)}\rangle + (-1)^m G_{op}(E + i\eta^{0+}) J_m(A/\omega) W |\varphi_{res}\rangle D \\ |\varphi_{cl}\rangle = D |\varphi_{res}\rangle \end{cases} \quad (9)$$

Where  $(-1)^m G_{op}(E + i\eta^{0+}) J_m(A/\omega) W |\varphi_{res}\rangle D$  describes the scattering contribution to the scattering state, which can be associated with the scattering amplitude  $f(\theta, k)$ . Besides, in the long-range approximation, the coordinate representation of the Green's function  $G_{op}$  takes the form:

$$G_{op}(E, \mathbf{r}, \mathbf{r}') \sim -\frac{(2\pi)^{3/2} \mu e^{ikr}}{2\pi\hbar^2} \frac{1}{r} [\varphi_{\mathbf{k}}^{(-)}(\mathbf{r}')]^*, \quad (10)$$

where  $\varphi_{\mathbf{k}}^{(-)}(\mathbf{r}') = [\varphi_{-\mathbf{k}}^{(+)}(\mathbf{r}')]^*$ .

In the low-momentum approximation, we may neglect higher partial-wave contributions to the scattering amplitude, rendering it isotropic. Furthermore, by substituting Eq. 10 into Eq. 4, we obtain:

$$f(\theta, k) = f_{bg}(\theta, k) - \frac{(2\pi)^3 \mu \langle \varphi_{\mathbf{k}}^{(-)} | (-1)^m J_m(A/\omega) W | \varphi_{res} \rangle}{2\pi\hbar^2} D \sim -a \quad (11)$$

On the other hand, the background scattering amplitude  $f_{bg}$  can be approximated by the background scattering length  $a_{BK}$ . Meanwhile, factor D can be represented as:

$$D = \frac{\langle \phi_{res} | (-1)^m J_m(A/\omega) W | \varphi_{\mathbf{k}}^{(+)} \rangle}{E - E_{res} - \langle \phi_{res} | J_m(A/\omega) W G_{op}(0) J_m(A/\omega) W | \phi_{res} \rangle}. \quad (12)$$

Therefore, by using the definition  $E_{res} = \hbar\omega_{cl} - m\hbar\omega$ , the s-scattering length can be expressed in the low-energy condition as

$$a = a_{BK} \left( 1 - \frac{\Delta_m}{-m\omega - \omega_0} \right), \quad (13)$$

or

$$\frac{1}{a} = \frac{1}{a_{BK}} \left( \frac{-m\omega - \omega_0}{-m\omega - \omega_0 - \Delta_m} \right), \quad (14)$$

where the resonance position is

$$\omega_o = -\omega_{cl} - \langle \phi_{res} | J_m(A/\omega) W G_{op}(0) J_m(A/\omega) W | \phi_{res} \rangle / \hbar, \quad (15)$$

and the width of the resonance is

$$\Delta_m = \frac{(2\pi)^3 \mu}{2\pi \hbar^3 a_{BK}} | \langle \phi_{res} | J_m(A/\omega) W | \varphi_0^{(+)} \rangle |^2. \quad (16)$$

### ANOTHER WAY TO UNDERSTAND THE MODULATION-INDUCED FESHBACH RESONANCE

Following the instance in [7], we develop another formal theory to understand the modulation-induced Feshbach resonance for our two-channel model. Starting with a Hamiltonian  $H = H_0 + V(t)$  with  $V(t+T) = V(t)$ , where  $T = \frac{2\pi}{\omega}$ ,  $\omega$  is the modulation frequency, we can apply the Floquet theory [8] and arrive at a set of coupled equations for the Floquet mode  $|\phi(t)\rangle = \sum_n e^{-i\omega_n t} |\phi_n\rangle$ ,

$$H_0 |\phi_n\rangle + \sum_s V_{n-s} |\phi_s\rangle = (\epsilon + \hbar\omega_n) |\phi_n\rangle, \quad (17)$$

where  $n$  is an integer,  $V_n$  is Fourier expansion of  $V(t)$ ,  $\omega_n = n\omega$ ,  $\epsilon$  is the quasi-energy of the Floquet state. The formal solution of the equation (17) is an infinitely coupled set of Lippmann-Schwinger equations,

$$|\phi_n\rangle = \delta_{n,0} |\phi_{in}\rangle + \frac{1}{\epsilon + \hbar\omega_n - H_0} \sum_s V_{n-s} |\phi_s\rangle, \quad (18)$$

where  $|\phi_{in}\rangle$  is the incoming state.

Based on this result, we choose the following two-channel Hamiltonian,

$$H_0 = H_{op} \otimes |op\rangle \langle op| + H_{cl} \otimes |cl\rangle \langle cl|, \quad (19)$$

$$V(t) = S(t) \otimes |cl\rangle \langle cl| + W \otimes |cl\rangle \langle op| + W \otimes |op\rangle \langle cl|, \quad (20)$$

where  $H_{op}$  and  $H_{cl}$  denote Hamiltonian for the open channel and the closed channel,  $W(r)$  is the coupling between them and  $S(t)$  is the periodically shaking term, and substitute equations (19), (20) to the equation (18) with the incoming state  $|\phi_{in}\rangle = |\varphi_{\mathbf{k}}^{(+)}\rangle$  and the general form of  $|\phi_n\rangle = |\phi_n^{op}\rangle \otimes |op\rangle + |\phi_n^{cl}\rangle \otimes |cl\rangle$ , we have

$$|\phi_n^{op}\rangle = \delta_{n,0} |\varphi_{\mathbf{k}}^{(+)}\rangle + \frac{1}{\epsilon + \hbar\omega_n - H_{op}} W |\phi_n^{cl}\rangle, \quad (21)$$

$$|\phi_n^{cl}\rangle = \frac{1}{\epsilon + \hbar\omega_n - H_{cl}} \sum_s V_{n-s} |\phi_s^{cl}\rangle + \frac{1}{\epsilon + \hbar\omega_n - H_{cl}} W |\phi_n^{op}\rangle. \quad (22)$$

The scattering amplitude for a transition from the incoming state to the 0th Floquet mode is determined by  $\langle \mathbf{r} | \phi_0^{op} \rangle$  when  $r \rightarrow \infty$ ,

$$f_0 = f_{bg} - \frac{\mu(2\pi)^3}{2\pi\hbar^2} \langle \varphi_{\mathbf{k}}^{(-)} | W | \phi_0^{cl} \rangle \sim -a, \quad (23)$$

where  $f_{bg}$  is the background scattering amplitude. With  $S(t) = \hbar A \cos(\omega t)$  as mentioned in the main text,  $V_n = \delta_{|n|,1} \hbar A$  and  $f_0$  will diverge when  $\epsilon + \hbar\omega_m - \hbar\omega_{cl}$  approaches 0, as  $\langle \varphi_{res} | \frac{1}{\epsilon + \hbar\omega_m - \hbar\omega_{cl}} | \varphi_{res} \rangle = (E - \hbar\omega_{cl} + \hbar\omega_m)^{-1}$ .

---

\* Electronic address: [cwlaser@ultracold.cn](mailto:cwlaser@ultracold.cn)

† Electronic address: [zhendongzhang19950715@gmail.com](mailto:zhendongzhang19950715@gmail.com)

‡ Electronic address: [hujiazhong01@ultracold.cn](mailto:hujiazhong01@ultracold.cn)

- [1] L. W. Clark, L.-C. Ha, C.-Y. Xu, and C. Chin, *Quantum dynamics with spatiotemporal control of interactions in a stable Bose-Einstein condensate*, Phys. Rev. Lett. 115, 155301 (2015).
- [2] Le Kien, F., Schneeweiss, P., Rauschenbeutel, A., *Dynamical polarizability of atoms in arbitrary light fields: general theory and application to cesium*, Eur. Phys. J. D 67, 92 (2013).
- [3] Wang, Jianmin and Dong, Liang and Wang, Xingchang and Zhou, Zihan and Huang, Jinshuai and Zuo, Ying and Siviloglou, Georgios A. and Chen, J. F., *Light-induced fictitious magnetic fields for quantum storage in cold atomic ensembles*, Phys. Rev. Research 6, L042002 (2024).
- [4] D.M. Bauer, M. Lettner, C. Vo, G. Rempe, and S. Dürr, *Control of a magnetic Feshbach resonance with laser light*, Nat. Phys. 5, 339 (2009).
- [5] Fu, Zhengkun and Wang, Pengjun and Huang, Lianghui and Meng, Zengming and Hu, Hui and Zhang, Jing, *Optical control of a magnetic Feshbach resonance in an ultracold Fermi gas*, PhysRevA.88.041601 (2013).
- [6] Kohler, Thorsten and Goral, Krzysztof and Julienne, Paul S, *Production of cold molecules via magnetically tunable Feshbach resonances*, Rev. Mod. Phys. 78, 1311 (2006).
- [7] D. H. Smith, *Inducing resonant interactions in ultracold atoms with a modulated magnetic field*, Phys. Rev. Lett. 115, 193002 (2015).
- [8] Martin Holthaus, *Floquet engineering with quasienergy bands of periodically driven optical lattices*, 2016 J. Phys. B: At. Mol. Opt. Phys. 49 013001.